

## Chapter 2

### Paper I—Rotation Periods of 12,000 Main-Sequence *Kepler* Stars

The content of this chapter has been published in Nielsen et al. (2013), A & A vol. 557, L10. The work was carried out and written by myself, under the supervision of L. Gizon, H. Schunker from the Max Planck Institute for Solar System Research and in collaboration with C. Karoff from Aarhus University, Denmark. The final section of the chapter is a summary of the progress that has been made in the field since the publication of Nielsen et al. (2013), with respect to measuring surface differential rotation and understanding the effects of spots on the observed light curves.

#### 2.1 Summary of Paper I

We aim to measure the starspot rotation periods of active stars in the *Kepler* field as a function of spectral type and to extend reliable rotation measurements from F-, G-, and K-type to M-type stars. Using the Lomb-Scargle periodogram we searched more than 1,50,000 stellar light curves for periodic brightness variations. We analyzed periods between 1 and 30 days in eight consecutive *Kepler* quarters, where 30 days is an estimated maximum for the validity of the PDC\_MAP data correction pipeline. We selected stable rotation periods, i.e., periods that do not vary from the median by more than one day in at least six of the eight quarters. We averaged the periods for each stellar spectral class according to B-V color and compared the results to archival  $v \sin i$  data, using stellar radii estimates from the *Kepler* Input Catalog. We report on the stable starspot rotation periods of 12151 *Kepler* stars. We find good agreement between starspot velocities and  $v \sin i$  data for all F-, G- and early K-type stars. The 795 M-type stars in our sample have a median rotation period of 15.4 days. We find an excess of M-type stars with periods less than 7.5 days that are potentially fast-rotating and fully convective. Measuring photometric variability in multiple *Kepler* quarters appears to be a straightforward and reliable way to determine the rotation periods of a large sample of active stars, including late-type stars.

## 2.2 Introduction

Measuring stellar rotation as a function of age and mass is essential to studies of stellar evolution (Maeder 2009) and stellar dynamos (Böhm-Vitense 2007; Reiners et al. 2012). Rotation can be measured at the surface of individual stars using either spectroscopy (e.g., Royer et al. 2004) or periodic variations in photometric light curves due to the presence of starspots (Mosser et al. 2009). On the Sun, sunspots and plage regions modulate the solar irradiance with periods close to the solar rotation period. Brightness variations are also seen in other stars and are commonly attributed to the presence of magnetic activity in the case of main-sequence cool dwarfs (e.g., Berdyugina 2005). Sunspots and solar active regions have lifetimes of days to weeks (rarely months) (Solanki 2003) and are reasonably good tracers of solar surface rotation at low latitudes. Starspots have been observed to persist for even longer periods (e.g., Strassmeier 2009), and they appear at high latitudes as well.

The *Kepler* mission (Borucki et al. 2010) has been monitoring the light emitted by more than  $10^5$  stars since its launch in 2009. Treating such an enormous number of stars obviously demands an automated approach. In this paper we present the results of a straightforward automated method for analyzing *Kepler* time series and detecting amplitude modulation due to stellar activity, with the aim of determining stellar rotation periods.

## 2.3 Measuring Stellar Rotation

### 2.3.1 *Kepler* photometry

We used white light time series with a cadence of 29.42 min from the NASA *Kepler* satellite. The data are released in segments of  $\sim 90$  days (quarters) through the Mikulski Archive for Space Telescopes<sup>1</sup> for a total sample of stars currently numbering  $\sim 190000$ . We used quarters 2 through 9 (two years of observations in total). The data was processed for cosmic rays and flat fielding prior to release. We used the version of the data that was corrected by the PDC\_MAP pipeline (Smith et al. 2012). The PDC\_MAP correction attempts to detect and remove systematic trends and instrumental effects, which are common to a large set of adjacent stars on the photometer. In addition, we used the most recent data from the msMAP correction pipeline (Thompson et al. 2013, where ‘ms’ stands for multi-scale) to check for consistency with PDC\_MAP.

From an initial sample of 192668 stars, we discarded targets that are known eclipsing binaries (Matijević et al. 2012), planet host stars as well as planet candidate host stars, and *Kepler* objects of interest (all lists are available through the MAST

---

<sup>1</sup><http://archive.stsci.edu/kepler/>.

portal). We do this to reduce the possibility of false positive detections, since these types of variability may be mistaken for transits of starspots.

### 2.3.2 Detecting Rotation Periods

Provided active regions or starspots are present over several rotations of the star, a peak will appear in the periodogram of the time series. Assuming starspots trace surface rotation, this provides a way to measure the rotation rate of the star at the (average) latitude of the starspots. Simulations by Nielsen and Karoff (2012) show that selecting the peak of maximum power is a suitable method for recovering the stellar rotation period.

We analyzed the *Kepler* observations as follows:

1. We compute a Lomb-Scargle (LS) periodogram (see Frandsen et al. 1995) for each star in each quarter for periods between 1 and 100 days, using PDC\_MAP data.
2. We find the peak of maximum power in this period range and record its period.
3. If the period of the peak falls between 1 and 30 days, we consider it due to stellar variability and not instrumental effects.
4. The peak height must be at least four times greater than the white noise estimated from the root mean square (RMS) of the time series (Kjeldsen and Bedding 1995).

The lower bound in periods of one day is set to avoid the hot g-mode pulsators with frequencies of a few cycles per day (see Aerts et al. 2010, Chap. 2). Some contamination from g-mode pulsations is expected for F- or earlier-type stars; however, we have not investigated how to automatically differentiate these pulsations from stellar activity variability. The upper bound in period of 30 days is the estimated limit for which the PDC\_MAP pipeline does not overcorrect the light curve, to the extent that it completely removes the intrinsic stellar signal (Thompson et al. 2013). We calculated periods up to 100 days to ensure that any peak found below 30 days is not a potential side lobe of a dominating long-term trend ( $>30$  days).

### 2.3.3 Selecting Stable Rotation Periods

Further, we require that the measured periods are stable over several *Kepler* quarters. Specifically,

5. We determine the median value of the measured periods over all eight quarters;
6. We select stars for which the median absolute deviation (MAD) of the measured periods is less than one day, i.e.,  $\text{MAD} < 1$  day; The MAD is defined as  $\text{MAD} = \langle |P_i - \langle P_i \rangle| \rangle$  (where  $\langle \rangle$  is the median).

7. From these, we select stars with six or more (out of eight) measured periods within 2 MAD of the median period;
8. We repeat this method using the msMAP data and flag stars that do not satisfy the above criteria.

We use the MAD since it is less sensitive to outliers than the standard deviation (Hoaglin et al. 2000). Requiring that a particular variation for a star is visible in multiple quarters reduces the risk of the detection coming from low-frequency noise from, say, instrumental effects. The LS periodogram is calculated at  $\sim 1300$  linearly spaced frequencies between  $1.2 \times 10^{-2}$  and  $3.9 \times 10^{-4}$  mHz ( $0.03 \text{ d}^{-1}$  and  $1 \text{ d}^{-1}$ ). The MAD limit of one day (point 6), along with the signal attenuation introduced by the PDC\_MAP correction, leads to a selection bias towards stars with shorter rotation periods. Examples of periods detected for three stars are shown in Fig. 2.1.

We applied the scaling relation by Kjeldsen and Bedding (2011) to find timescales for p-mode pulsations in cool main sequence stars and red giants. We found that stars with  $\log g \lesssim 2$  have pulsation periods that can potentially overlap with the range investigated in this work. We opted for a conservative approach and discarded stars with  $\log g < 3.4$  to remove red giants from the sample. Following the scaling relation, the main sequence stars were found to have pulsation timescales from minutes to hours, far below our lower period limit. Once all the above criteria are met, the rotation period,  $P_{\text{rot}}$ , is defined as the median of the valid periods. This selection process leaves us with 12151 stars out of the original sample of 192668. When using the msMAP data, we find that  $\sim 80\%$  of these stars satisfy the above criteria as well. Of these, 0.9% differ from the PDC\_MAP results by more than one resolution

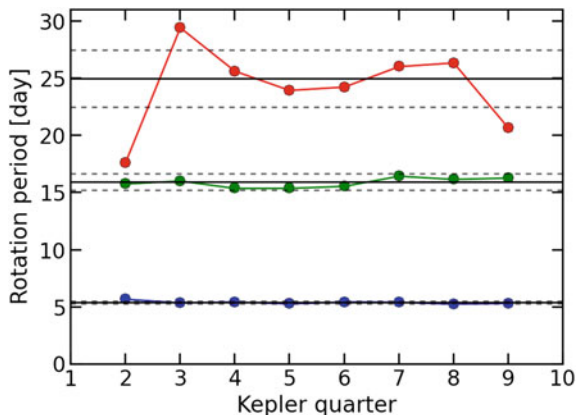


**Fig. 2.1** Measured periods in each quarter of observation for three *Kepler* stars (red, green and blue). The solid line is the median period over all quarters for each star. The dashed horizontal lines indicate two median absolute deviations (MAD) from the median period. The long period target (red) is discarded by the algorithm due to high scatter in the period measurements ( $\text{MAD} = 1.26$  days). The green and blue target are examples of stars that meet the selection criteria. Reproduced with permission from Astronomy & Astrophysics, © ESO

element, predominantly because the msMAP data shows the first harmonic instead of the fundamental period of the variability. The msMAP pipeline treats the long periods ( $P_{\text{rot}} \lesssim 15$  days) differently than the PDC\_MAP (see Thompson et al. 2013).

The results for all 12151 stars are shown in Table 1,<sup>2</sup> which is provided as online material through the CDS. Column 1 gives the *Kepler* Input Catalog (KIC) name of the star, cols. 2 and 3 are the rotation period and scatter (MAD), and cols. 4 to 8 give the  $g - r$  color,  $E(B - V)$ , radius,  $\log g$ , and  $T_{\text{eff}}$ , respectively, all of which are KIC values. Column 9 is a flag indicating whether each msMAP-corrected data set satisfies the criteria of Sect. 2.3. Column 10 gives the msMAP period of the stars where we find rotation rates from the two data sets that differ by more than one resolution element.

## 2.4 Consistency with $v \sin i$ Measurements

We performed a rudimentary spectral classification of the stars based on their  $B - V$  color indices. The KIC provides  $g - r$  values that we converted to  $B - V$  using the relation  $B - V = 0.98 (g - r) + 0.22$  given by Jester et al. (2005) for stars with R-I color indices  $< 1.15$ . The  $B - V$  values are dereddened using the  $E(B - V)$  values from the KIC (see Brown et al. 2011, for details on their derivation). The calculated  $B - V$  colors are mapped to a spectral type as per Gray (2005, Appendix B).

We compared the periods found in this work with  $v \sin i$  values compiled by Glebocki and Gnacinski (2005). This list contains  $v \sin i$  values and spectral types for  $\sim 30000$  cluster stars almost isotropically distributed in galactic coordinates. Using our approximate spectral classification we compared the median equatorial velocities of this sample with our results from the *Kepler* targets. From the  $v \sin i$  sample we select stars with apparent V magnitude from 6 to 15, roughly equivalent to the magnitude range of the *Kepler* targets. We discard any stars from the  $v \sin i$  sample that have been ambiguously labeled as ‘uncertain’. Lastly, we select only dwarf stars since this is the main constituent of the stars selected by our method, reducing the  $v \sin i$  sample to be comparable in number to our *Kepler* target list.

For each spectral type (s.t.) in our sample of *Kepler* targets we calculate the median equatorial rotational velocity by  $\bar{v}(\text{s.t.}) = 2\pi \langle R_{\text{KIC}}/P_{\text{rot}} \rangle$  where  $\langle \rangle$  denotes the median over stars with spectral type s.t.,  $R_{\text{KIC}}$  is the KIC stellar radius, and  $P_{\text{rot}}$  is the rotation period determined by our algorithm. The KIC radii are notoriously bad estimates in some cases; however, by comparing these with characteristic radii given in Gray (2005, Appendix B) we find that the median values in the region of F0 to K0 agree within  $\sim 15\%$ . Outside this range of spectral types the radii are initially overestimated, but become strongly underestimated for A-type stars and earlier.

Since we have such a large statistical sample of  $v \sin i$  measurements within each spectral type, a random distribution of inclinations of rotation axes gives  $\langle \sin i \rangle = \pi/4$  (e.g., Gray 2005). Therefore the median equatorial velocity for a given spectral

<sup>2</sup><http://cdsarc.u-strasbg.fr/viz-bin/qcat?J/A+A/557/L10>.

type can be approximated by  $(4/\pi) \langle v \sin i \rangle$ , which is directly comparable to the  $\bar{v}(s.t.)$  computed for the *Kepler* targets.

Panel A in Fig. 2.2 shows clear agreement, from late A-type to early G-type stars, between the median equatorial velocities of the  $v \sin i$  sample and those we derived from our measured *Kepler* rotation periods. For additional comparison we included the  $v \sin i$  measurements from Reiners and Mohanty (2012), where the horizontal bar represents 201 stars with velocities below 4 km/s. Panel B shows our measured

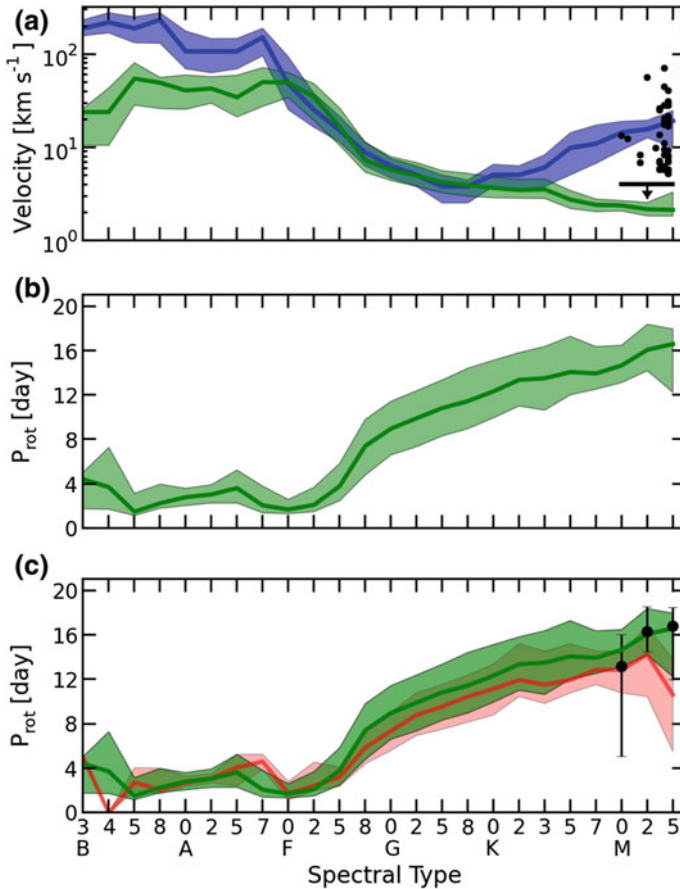


**Fig. 2.2** Panel A The blue curve is the median equatorial velocity  $(4/\pi) \langle v \sin i \rangle$  for each spectral type from Glebocki and Gnacinski (2005). The green curve shows the equatorial velocity of the *Kepler* targets,  $\bar{v}(s.t.)$ , derived from the measured rotation periods and the KIC radii. The black points show measurements by Reiners and Mohanty (2012). In this sample 201 stars have an upper  $v \sin i$  limit of 4 km/s (due to instrumental limitations), these stars are represented by the solid bar. Panel B The rotation periods  $P_{\text{rot}}$  of the stars in our sample, averaged within each spectral type. Panel C The same as panel B, but for comparison we show the median of the rotation periods measured by McQuillan et al. (2013) (black points with errorbars), for the stars overlapping with our sample. Similarly, the red curve shows the median of the rotation periods found by Debosscher et al. (2011). Shaded areas and error bars span the upper and lower 34th percentile values from the median. Reproduced with permission from Astronomy & Astrophysics, © ESO

rotation periods  $P_{\text{rot}}$ , as a function of spectral type, which we used to calculate the equatorial velocities. We also calculated the median periods of the *Kepler* stars found in Debosscher et al. (2011) and McQuillan et al. (2013) that are present in our sample. These are shown in comparison to our results in panel C. We find that  $\sim 96\%$  and  $\sim 97\%$  of their measured rotation rates fall within one frequency resolution element ( $1/90 \text{ d}^{-1}$ ) of our values for the corresponding stars.

## 2.5 Rotation of Late Type Stars

Owing to their small radius and long rotation period, the  $v \sin i$  measurements of late type stars are limited by spectral resolution. The  $v \sin i$  measurements of Reiners and Mohanty (2012) have a lower limit at  $\sim 4 \text{ km/s}$ . The KIC radii are overestimated for stars later than K0 so our velocities are therefore upper limits, but we still systematically find rotation slower than  $\sim 4 \text{ km/s}$ . This places our measurements at or below the lower limit for spectroscopically determining rotation for these types of stars.

The late M-type stars are of particular interest since they represent the transition from solar-like convective envelopes to fully convective interiors. Figure 2.3 shows the distributions of stars that have been classified as M-type, found in this work and those by McQuillan et al. (2013). The median of the distribution in our sample is 15.4 days. There appears to be good agreement with the result of McQuillan et al. (2013). We note an excess of fast rotators with  $P < 7.5$  days. The study by Reiners and Mohanty (2012) shows that the number of magnetically active M-type dwarfs increases approximately after spectral subtype M3, which appears correlated with an increase in the number of fast rotators (see top panel of Fig. 2.2), likely

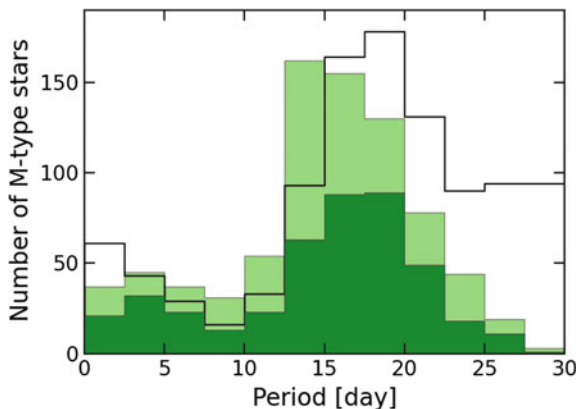


**Fig. 2.3** The light green histogram shows the distribution of rotation periods for the 795 M-type stars in our sample (median, 15.4 days). For comparison the black line shows the results by McQuillan et al. (2013) for periods less than 30 days. The dark-green histogram shows the distribution of rotation periods measured by McQuillan et al. (2013) for the stars in common with our sample. Reproduced with permission from Astronomy & Astrophysics, © ESO

marking the transition to full convection. Our sample contains 795 M-type stars, where  $\sim 15\%$  have periods less than 7.5 days; i.e., these are potentially fast-rotating, fully convective M-type dwarfs, such as those found by Reiners and Mohanty (2012). As a result of the KIC  $\log g$  having errors of approximately  $\pm 0.4$  dex (Brown et al. 2011), the sample probably still contains some cool giants. A visual inspection of the power spectra of the M-type stars, with periods  $P < 7.5$  days, indicated that 3 out of 119 stars had p-mode pulsations that could potentially be misidentified as periodic activity. Thus the contamination by p-mode pulsations appears to be negligible. A more rigorous determination of  $\log g$  and spectral type for these stars is required to distinguish stellar evolutionary stages. However, even a fraction of our sample of M-type dwarfs still significantly complements the existing literature on this critical region for understanding differences in stellar dynamos.

## 2.6 Conclusions

We developed a straightforward, automated method for detecting stable rotation periods for a large sample of *Kepler* targets. A total of 12151 stars ranging from spectral type B3 to M5 all show recurring periods in at least six of the eight quarters of analyzed *Kepler* data. This, along with the requirement that the stars in question have a maximum MAD of one day, are empirically determined criteria. Using the KIC stellar radii, we found very good agreement between the equatorial rotational velocities derived from the *Kepler* rotation periods and independent  $v \sin i$  measurements for F0 to K0 type stars. For later type stars we find an inconsistency with the Glebocki and Gnacinski (2005) catalog. This is due to an age difference between the two samples, since the Glebocki and Gnacinski (2005) catalog mainly consists of young open cluster stars. However, our results for M-type stars agree well with those reported by Reiners and Mohanty (2012) and McQuillan et al. (2013). The study by Debosscher et al. (2011) analyzed a different set of *Kepler* data, but we still find good agreement with the stars overlapping with our sample.

We have primarily studied stars that have long-lived stellar activity signatures. We tested our method on solar-disk integrated light at solar maximum (January 2001 to March 2003), observed by the VIRGO instrument aboard SOHO (Frohlich et al. 1997). The VIRGO green channel data were divided into 90-day segments, and we applied the method described in Sect. 2.3. The stability criterion was not met due to a period scatter of  $\text{MAD} = 3.7$  days. Analysis of other segments of VIRGO data from 1995 to 2013 also resulted in rejection. This shows that stars with solar-like (low) activity are rejected from our sample; for such stars, rotation period measurements are too noisy and not stable enough over time. A further bias is the upper limit of  $P \leq 30$  days chosen because the PDC\_MAP does not yield reliable corrections for longer periods. An obvious improvement to our analysis would be to investigate ways of increasing this upper limit, for a complete view of slow rotators.



As expected, we found that hot stars rotate faster than their cooler counterparts (Barnes 2003; Kraft 1970). The rotation periods of hot stars should be treated with some caution since they may be false positives from g-mode pulsations. Nevertheless, our analysis method detects periodic variations in brightness that satisfy the selection criteria. The measured variability is not necessarily of magnetic origin, but could arise from, for example, chemical surface inhomogeneities in chemically peculiar hot stars. Chemical spots can produce photometric variability that traces the stellar rotation (Wraight et al. 2012; Paunzen et al. 2013). The short periods measured for the early spectral types (see Fig. 2.2) in our sample are therefore not contradictory to the expected fast rotation of hot stars (Royer et al. 2004).

This work is only one step toward characterizing of the rotation of stars in the *Kepler* field. *Kepler* photometry is proving very useful in adequately sampling the slow rotation rates of cool, faint stars. Future work will include detailed starspot modeling in order to measure latitudinal differential rotation (Reinhold and Reiners 2013) and asteroseismology (e.g., Deheuvels et al. 2012) to infer internal differential rotation. The *Kepler* observations offer unique possibilities for calibrating the mass-age-color relations in gyrochronology (Skumanich 1972; Barnes 2007) and exploring the close relation between stellar rotation and activity cycles.

## 2.7 Further Discussion of Chap. 1

Since the publication of Nielsen et al. (2013) there have been a number of studies on the topic of stellar rotation from surface variability. Aigrain et al. (2015) summarizes these very well in a hare-and-hound exercise, where numerous teams participated in an attempt to discern how well various parameters can be extracted from the *Kepler* light curves. Synthetic light curves were produced using a spot model which included: an activity cycle, a solar-like butterfly diagram, differential rotation, spot evolution, and multiple spots. Of the 1000 generated light curves, 770 were injected into 'quiet' *Kepler* light curves, in order to simulate the systematic noise generated by the spacecraft, while the remaining were either noise-less spot models or solar irradiance time series based on VIRGO observations.

The teams included members with previously developed methods for spot analysis which are summarized here. Each method has advantages and disadvantages, as illustrated by the detection and false-positive rates.

- Peak detection in the Lomb-Scargle periodogram was employed in Nielsen et al. (2013) (as described above), and in Reinhold and Reiners (2013) who simultaneously attempted to extract estimates of differential rotation from the periodogram. The results of these methods showed that while the method by Nielsen et al. (2013) had the lowest detection rate ( $\sim 15\%$ ) of all the methods, it was the only method with a 0% false-positive rate, i.e., all the detected periods matched the input values. The method by Reinhold and Reiners (2013) (also automated) had a significantly

higher detection rate of  $\sim 66\%$ , but subsequently also had a higher false positive rate of  $\sim 25\%$ .

- The autocorrelation function (ACF) was used in McQuillan et al. (2014). This method was designed to automatically search for the peak in the ACF corresponding to the rotation period, based on an evaluation system using the effective temperature of the star and the period of the variability to reduce contamination from potential pulsating stars. This method detected a total of 34030 stars in the original *Kepler* sample, which to date is the largest homogeneous catalog of rotation periods.

An additional team used the ACF to measure periodicity, using a previously unpublished method which incorporated Savitzky-Golay filtering (Savitzky and Golay 1964). Both teams using the ACF reported very high detection rates of 100% and 95% respectively, but similar to Reinhold and Reiners (2013) the false-positive rate was around  $\sim 30\%$ .

- Direct spot modeling as described in Lanza et al. (2014) was also applied to the test sample. However, this proved be very time consuming and computationally expensive, and so only about half the sample was analyzed, which yielded an detection rate of 27% and a false-positive rate of  $\sim 30\%$ .
- Another team used the method shown in García et al. (2014), which is based on a wavelet analysis of the time series. This method uses a Morlet wavelet, which consists of a sinusoidal signal with a Gaussian amplitude modulation, and generates a time-frequency spectrum of the time series. This method can account for the non-sinusoidal shape of the spot transit signal, thereby minimizing the risk of identifying harmonic peaks in the periodogram (Mathur et al. 2010). Combining this with the ACF method, this team reported the best combination of high detection rate and low false-positive rate (79% and 12% respectively), although Aigrain et al. (2015) note that this team were not fully blinded in the hare-and-hound exercise.

The majority of these methods revolve around decomposing the time series into its constituent frequencies. This makes the detection of a rotation period relatively simple and straight-forward, illustrated by the high detection rate and moderately low false-positive rates, as well as the fact that these methods are almost completely automated. This makes them well suited for treating large samples of data from, e.g., the *Kepler* mission or the upcoming TESS and PLATO missions. However, any further information about latitudinal differential rotation and spot lifetime cannot reliably be inferred using these methods. None of the tested methods could recover the input values of these two quantities; surprisingly, even the attempts at directly modeling the spot signature in the light curves failed in this respect.

This suggests that some form of prior information about the star is necessary in order to constrain these two quantities. For Sun-like stars this could potentially come from asteroseismology, which in many cases can provide a good estimate of the inclination of the rotation axis (see Sect. 1.2.4.2). This information can be used in spot modeling efforts to constrain the otherwise unknown spot latitude, since these two parameters are otherwise degenerate. The spot latitude is in turn necessary for determining the latitudinal differential rotation coefficients. Asteroseismology may

also be applied to place limits directly on the latitudinal differential rotation. Since the latitudinal differential rotation and the spot lifetime are degenerate in the LSP and the ACF, a constraint on the differential rotation from asteroseismology could then potentially be used to place limits on the spot lifetime.

## References

- C. Aerts, J. Christensen-Dalsgaard, D.W. Kurtz. *Asteroseismology* (2010)
- S. Aigrain, J. Llama, T. Ceillier, M.L.D. Chagas, J.R.A. Davenport, R.A. García, K.L. Hay, A.F. Lanza, A. McQuillan, T. Mazeh, J.R. de Medeiros, M.B. Nielsen, T. Reinhold, Testing the recovery of stellar rotation signals from Kepler light curves using a blind hare-and-hounds exercise. *MNRAS* **450**, 3211–3226 (2015). doi:[10.1093/mnras/stv853](https://doi.org/10.1093/mnras/stv853)
- S.A. Barnes, On the rotational evolution of solar- and late-type stars, its magnetic origins, and the possibility of stellar gyrochronology. *ApJ* **586**, 464–479 (2003). doi:[10.1086/367639](https://doi.org/10.1086/367639)
- S.A. Barnes, Ages for illustrative field stars using gyrochronology: viability, limitations, and errors. *ApJ* **669**, 1167–1189 (2007). doi:[10.1086/519295](https://doi.org/10.1086/519295)
- S.V. Berdyugina, Starspots: a key to the stellar dynamo. *Living Rev. Solar Phys.* **2**, 8 (2005). doi:[10.12942/lrsp-2005-8](https://doi.org/10.12942/lrsp-2005-8)
- E. Böhm-Vitense, Chromospheric activity in G and K main-sequence stars, and what it tells us about stellar dynamos. *ApJ* **657**, 486–493 (2007). doi:[10.1086/510482](https://doi.org/10.1086/510482)
- W.J. Borucki, D. Koch, G. Basri, N. Batalha, T. Brown, D. Caldwell, J. Caldwell, J. Christensen-Dalsgaard, W.D. Cochran, E. DeVore, E.W. Dunham, A.K. Dupree, T.N. Gautier, J.C. Geary, R. Gilliland, A. Gould, S.B. Howell, J.M. Jenkins, Y. Kondo, D.W. Latham, G.W. Marcy, S. Meibom, H. Kjeldsen, J.J. Lissauer, D.G. Monet, D. Morrison, D. Sasselov, J. Tarter, A. Boss, D. Brownlee, T. Owen, D. Buzasi, D. Charbonneau, L. Doyle, J. Fortney, E.B. Ford, M.J. Holman, S. Seager, J.H. Steffen, W.F. Welsh, J. Rowe, H. Anderson, L. Buchhave, D. Ciardi, L. Walkowicz, W. Sherry, E. Horch, H. Isaacson, M.E. Everett, D. Fischer, G. Torres, J.A. Johnson, M. Endl, P. MacQueen, S.T. Bryson, J. Dotson, M. Haas, J. Kolodziejczak, J. Van Cleve, H. Chandrasekaran, J.D. Twicken, E.V. Quintana, B.D. Clarke, C. Allen, J. Li, H. Wu, P. Tenenbaum, E. Verner, F. Bruhweiler, J. Barnes, A. Prsa, Kepler planet-detection mission: introduction and first results. *Science* **327**, 977 (2010). doi:[10.1126/science.1185402](https://doi.org/10.1126/science.1185402)
- T.M. Brown, D.W. Latham, M.E. Everett, G.A. Esquerdo, Kepler input catalog: photometric calibration and stellar classification. *AJ* **142**, 112 (2011). doi:[10.1088/0004-6256/142/4/112](https://doi.org/10.1088/0004-6256/142/4/112)
- J. Debosscher, J. Blomme, C. Aerts, J. De Ridder, Global stellar variability study in the field-of-view of the Kepler satellite. *A & A* **529**, A89 (2011). doi:[10.1051/0004-6361/201015647](https://doi.org/10.1051/0004-6361/201015647)
- S. Deheuvels, R.A. García, W.J. Chaplin, S. Basu, H.M. Antia, T. Appourchaux, O. Benomar, G.R. Davies, Y. Elsworth, L. Gizon, M.J. Goupil, D.R. Reese, C. Regulo, J. Schou, T. Stahn, L. Casagrande, J. Christensen-Dalsgaard, D. Fischer, S. Hekker, H. Kjeldsen, S. Mathur, B. Mosser, M. Pinsonneault, J. Valenti, J.L. Christiansen, K. Kinemuchi, F. Mullally, Seismic evidence for a rapidly rotating core in a lower-giant-branch star observed with Kepler. *ApJ* **756**, 19 (2012). doi:[10.1088/0004-637X/756/1/19](https://doi.org/10.1088/0004-637X/756/1/19)
- S. Frandsen, A. Jones, H. Kjeldsen, M. Viskum, J. Hjorth, N.H. Andersen, B. Thomsen, CCD photometry of the  $\delta$ -Scuti star  $\kappa^2$  Bootis. *A & A* **301**, 123 (1995)
- C. Frohlich, B.N. Andersen, T. Appourchaux, G. Berthomieu, D.A. Crommelynck, V. Domingo, A. Fichtot, W. Finsterle, M.F. Gomez, D. Gough, A. Jimenez, T. Leifsen, M. Lombaerts, J.M. Pap, J. Provost, T.R. Cortes, J. Romero, H. Roth, T. Sekii, U. Telljohann, T. Toutain, C. Wehrli, First results from VIRGO, the experiment for helioseismology and solar irradiance monitoring on SOHO. *Sol. Phys.* **170**, 1–25 (1997). doi:[10.1023/A:1004969622753](https://doi.org/10.1023/A:1004969622753)

- R.A. García, T. Ceillier, D. Salabert, S. Mathur, J.L. van Saders, M. Pinsonneault, J. Ballot, P.G. Beck, S. Bloemen, T.L. Campante, G.R. Davies, J.-D. do Nascimento, Jr., S. Mathis, T.S. Metcalfe, M.B. Nielsen, J.C. Suárez, W.J. Chaplin, A. Jiménez, C. Karoff, Rotation and magnetism of *Kepler* pulsating solar-like stars. Towards asteroseismically calibrated age-rotation relations. *A & A* **572**, A34 (2014). doi:[10.1051/0004-6361/201423888](https://doi.org/10.1051/0004-6361/201423888)
- R. Glebocki, P. Gnacinski, *VizieR* online data catalog: catalog of stellar rotational velocities (Glebocki+ 2005). *VizieR Online Data Catalog* **3244** (2005)
- D.F. Gray, *The Observation and Analysis of Stellar Photospheres* (2005)
- D.C. Hoaglin, F. Mosteller, J.W. Tukey, *Understanding Robust and Exploratory Data Analysis*, Wiley class edition. Wiley (2000). ISBN 978-0-471-38491-5
- S. Jester, D.P. Schneider, G.T. Richards, R.F. Green, M. Schmidt, P.B. Hall, M.A. Strauss, D.E. Vanden Berk, C. Stoughton, J.E. Gunn, J. Brinkmann, S.M. Kent, J.A. Smith, D.L. Tucker, B. Yanny, The sloan digital sky survey view of the palomar-green bright quasar survey. *AJ* **130**, 873–895 (2005). doi:[10.1086/432466](https://doi.org/10.1086/432466)
- H. Kjeldsen, T.R. Bedding, Amplitudes of stellar oscillations: the implications for asteroseismology. *A & A* **293**, 87–106 (1995)
- H. Kjeldsen, T.R. Bedding, Amplitudes of solar-like oscillations: a new scaling relation. *A & A* **529**, L8 (2011). doi:[10.1051/0004-6361/201116789](https://doi.org/10.1051/0004-6361/201116789)
- R.P. Kraft. *Stellar Rotation* (1970), p. 385
- A.F. Lanza, M.L. Das Chagas, J.R. De Medeiros, Measuring stellar differential rotation with high-precision space-borne photometry. *A & A* **564**, A50 (2014). doi:[10.1051/0004-6361/201323172](https://doi.org/10.1051/0004-6361/201323172)
- A. Maeder, *Physics. Form. Evol. Rotating Stars* (2009). doi:[10.1007/978-3-540-76949-1](https://doi.org/10.1007/978-3-540-76949-1)
- S. Mathur, R.A. García, C. Régulo, O.L. Creevey, J. Ballot, D. Salabert, T. Arentoft, P.-O. Quirion, W.J. Chaplin, H. Kjeldsen, Determining global parameters of the oscillations of solar-like stars. *A & A* **511**, A46 (2010). doi:[10.1051/0004-6361/200913266](https://doi.org/10.1051/0004-6361/200913266)
- G. Matijević, A. Prša, J.A. Orosz, W.F. Welsh, S. Bloemen, T. Barclay, *Kepler* eclipsing binary stars. III. Classification of *Kepler* eclipsing binary light curves with locally linear embedding. *AJ* **143**, 123 (2012). doi:[10.1088/0004-6256/143/5/123](https://doi.org/10.1088/0004-6256/143/5/123)
- A. McQuillan, S. Aigrain, T. Mazeh, Measuring the rotation period distribution of field M dwarfs with *Kepler*. *MNRAS* **432**, 1203–1216 (2013). doi:[10.1093/mnras/stt536](https://doi.org/10.1093/mnras/stt536)
- A. McQuillan, T. Mazeh, S. Aigrain, Rotation periods of 34,030 *Kepler* main-sequence stars: the full autocorrelation sample. *ApJS* **211**, 24 (2014). doi:[10.1088/0067-0049/211/2/24](https://doi.org/10.1088/0067-0049/211/2/24)
- B. Mosser, F. Baudin, A.F. Lanza, J.C. Huelot, C. Catala, A. Baglin, M. Auvergne, Short-lived spots in solar-like stars as observed by CoRoT. *A & A* **506**, 245–254 (2009). doi:[10.1051/0004-6361/200911942](https://doi.org/10.1051/0004-6361/200911942)
- M.B. Nielsen, L. Gizon, H. Schunker, C. Karoff, Rotation periods of 12 000 main-sequence *Kepler* stars: Dependence on stellar spectral type and comparison with  $v \sin i$  observations. *A & A* **557**, L10 (2013). doi:[10.1051/0004-6361/201321912](https://doi.org/10.1051/0004-6361/201321912)
- M.B. Nielsen, C. Karoff, Starspot simulations for *Kepler*. *Astronomische Nachrichten* **333**, 1036 (2012). doi:[10.1002/asna.201211817](https://doi.org/10.1002/asna.201211817)
- E. Paunzen, K.T. Wraight, L. Fossati, M. Netopil, G.J. White, D. Bewsher, A photometric study of chemically peculiar stars with the STEREO satellites—II. Non-magnetic chemically peculiar stars. *MNRAS* **429**, 119–125 (2013). doi:[10.1093/mnras/sts318](https://doi.org/10.1093/mnras/sts318)
- A. Reiners, N. Joshi, B. Goldman, A catalog of rotation and activity in early-m stars. *AJ* **143**, 93 (2012). doi:[10.1088/0004-6256/143/4/93](https://doi.org/10.1088/0004-6256/143/4/93)
- A. Reiners, S. Mohanty, Radius-dependent Angular Momentum Evolution in Low-mass Stars. I. *ApJ* **746**, 43 (2012). doi:[10.1088/0004-637X/746/1/43](https://doi.org/10.1088/0004-637X/746/1/43)
- T. Reinhold, A. Reiners, Fast and reliable method for measuring stellar differential rotation from photometric data. *A & A* **557**, A11 (2013). doi:[10.1051/0004-6361/201321161](https://doi.org/10.1051/0004-6361/201321161)
- F. Royer, J. Zorec, A.E. Gómez, Rotational velocity distributions of A-type stars, in *The A-Star Puzzle*, ed. by J. Zverko, J. Ziznovsky, S.J. Adelman, W.W. Weiss, *IAU Symposium*, vol. 224 (2004), pp. 109–114. doi:[10.1017/S1743921304004442](https://doi.org/10.1017/S1743921304004442)

- A. Savitzky, M.J.E. Golay, Smoothing and differentiation of data by simplified least squares procedures. *Anal. Chem.* **36**, 1627–1639 (1964)
- A. Skumanich, Time scales for CA II emission decay, rotational braking, and lithium depletion. *ApJ* **171**, 565 (1972). doi:[10.1086/151310](https://doi.org/10.1086/151310)
- J.C. Smith, M.C. Stumpe, J.E. Van Cleve, J.M. Jenkins, T.S. Barclay, M.N. Fanelli, F.R. Girouard, J.J. Kolodziejczak, S.D. McCauliff, R.L. Morris, J.D. Twicken, Kepler presearch data conditioning II—A Bayesian approach to systematic error correction. *PASP* **124**, 1000–1014 (2012). doi:[10.1086/667697](https://doi.org/10.1086/667697)
- S.K. Solanki, Sunspots: an overview. *A & A* **11**, 153–286 (2003). doi:[10.1007/s00159-003-0018-4](https://doi.org/10.1007/s00159-003-0018-4)
- K.G. Strassmeier, Starspots. *A & A* **17**, 251–308 (2009). doi:[10.1007/s00159-009-0020-6](https://doi.org/10.1007/s00159-009-0020-6)
- S.E. Thompson, J.L. Christiansen, J.M. Jenkins, D.A. Caldwell, T. Barclay, S.T. Bryson, C.J. Burke, J.R. Campbell, J. Catanzarite, B.D. Clarke, J.L. Coughlin, F. Girouard, M.R. Haas, K. Ibrahim, T.C. Klaus, J.J. Kolodziejczak, J. Li, S.D. McCauli, R. Morris, F. Mullally, E.V. Quintana, J. Rowe, A. Sabale, S. Seader, J.C. Smith, M.D. Still, P.G. Tenenbaum, J.D. Twicken, A.K. Uddin, Kepler Data Release 21 Notes (KSCI-19061-001). Technical Report (2013)
- K.T. Wraight, L. Fossati, M. Netopil, E. Paunzen, M. Rode-Paunzen, D. Bewsher, A.J. Norton, G.J. White, A photometric study of chemically peculiar stars with the STEREO satellites—I. Magnetic chemically peculiar stars. *MNRAS* **420**, 757–772 (2012). doi:[10.1111/j.1365-2966.2011.20090.x](https://doi.org/10.1111/j.1365-2966.2011.20090.x)

Differential Rotation in Sun-like Stars from Surface  
Variability and Asteroseismology

Nielsen, M.B.

2017, XVI, 101 p. 29 illus., 18 illus. in color., Hardcover

ISBN: 978-3-319-50988-4